Pis'ma v ZhETF, vol. 95, iss. 8, pp. 481 – 485 © 2012 April 25

Quantum Effects for Parametric X-ray Radiation during Channeling: Theory and First Experimental Observation

K. B. Korotchenko[1)], *Yu. L. Pivovarov*, *Y. Takabayashi*[+]

Department of Theoretical and Experimental Physics, National Research Tomsk Polytechnic University, 634050 Tomsk, Russia

[+]*SAGA Light Source, 8-7 Yayoigaoka, Tosu, Saga 841-0005, Japan*

Submitted 16 March 2012

The theory of x-ray radiation from relativistic channeled electrons at the Bragg angles – parametric x-radiation (PXR) during channeling (PXRC) – is developed while accounting for two quantum effects: the initial population of bound states of transverse motion and the transverse "form-factor" of channeled electrons. An experiment was conducted using a 255 MeV electron beam from a linac at the SAGA Light Source. We have identified a difference in the angular distributions of PXR and PXRC and obtained a fairly good agreement between the theoretical and experimental results.

1. Introduction. Parametric x-radiation from relativistic particles (PXR) arises during penetration of relativistically charged particles through a crystal target at large (Bragg) angles with respect to the particle velocity. As a rule, the trajectory is considered as a straight-line and the velocity vector is constant during penetration through the crystal. In this approach, PXR arises as the diffraction of virtual photons associated with the electromagnetic field of relativistic particles on the periodically arranged crystallographic planes. If an incident particle (below, we will discuss the case of electrons) is captured into a channeling regime, only the component of its momentum parallel to the channeling plane (axis) is constant, while the transverse motion is described by a solution of the classical equation of motion or the Schrödinger equation using the corresponding continuous planar or axial potential. As such, the PXR theory should be modified to take into account the channeling effect.

From a quantum perspective, if the solutions of the Schrödinger 1D (planar channeling) or 2D (axial channeling) equation are found (i.e., the wave functions of channeling states are calculated) and solutions of the Maxwell equations for x-rays in a crystal are known (e.g., in the 2-wave approximation), then the probabilities and angular distributions of x-radiation arising at possible transitions between various quantum channeling states can be calculated. Let us denote the initial quantum state of the channeled electron as i and the final state as f. By following the two first important theories [1, 2] the following classification of radiative transitions can be established.

1. Transitions $i \to f$ $(i \neq f)$ correspond to the so called diffracted channeling radiation (DCR). For this case, the possibility of DCR was discussed first in Ref. [1]. The kinematical theory of DCR was proposed in Refs. [2] and [3]. Later, the dynamical theory of DCR within the dipole approximation was developed for the case of planar channeling in Ref. [4]. In our previous reports [5–7], the theory of DCR in the dipole approximation was modified to take into account the band structure of transverse energy levels of channeled electrons and positrons.

2. Transitions with $i = f$ correspond to so-called parametric x-radiation during channeling (PXRC). This is a very specific case of DCR, which has not been studied in detail to date.

If the angle of incidence with respect to the channeling planes (axes) is greater than the Lindhard critical angle θ_L for channeling, the sub-barrier quantum states are not populated and the formulae for PXRC transform into the well known formulae for PXR [4].

2. PXRC – general theory. The aim of this Letter is to extend the qualitative consideration of earlier works [1, 2] and develop a more detailed theory of PXRC, and apply this theory to explain the very recent experimental data obtained using a 20 μm Si crystal and a 255 MeV electron beam from an injector linac at the SAGA Light Source (SAGA-LS) in Japan.

The matrix element for PXRC was obtained in Ref. [4]. This matrix element was modified to take into account the band structure of transverse energy levels of channeled electrons and avoid the dipole approximation, and has the form:

$$M_{nn}^{(-g)\tau} = \frac{\mathbf{i}e(2\pi/L)^N A_{0\kappa}^{*\tau}}{mc\gamma\sqrt{(1+W_\tau^2)}}(\boldsymbol{\varepsilon}_{g\tau}\mathbf{p})_\parallel F_{nn} \times \\ \times \delta(\mathbf{p}_\parallel - \mathbf{p}_\parallel^{'} - \hbar(\boldsymbol{\kappa}-\mathbf{g})_\parallel), \quad (1)$$

[1)] e-mail: korotchenko@tpu.ru

where n is the number of quantum states, L is the normalization length ($N = 1$ for axial channeling and $N = 2$ for planar channeling), $A^{*\tau}_{0\kappa}$ is the photon wave function, $\mathbf{p}_\parallel$ and $\mathbf{p}'_\parallel$ are the longitudinal electron momentum vectors before and after radiation, respectively, $\mathbf{g}$ is the reciprocal lattice vector, $\tau = (\pi, \sigma)$ is an index that indicates the components of the photon polarization vector $\boldsymbol{\varepsilon}_{g\tau}$ (if $\boldsymbol{\varepsilon}_{g\tau}$ is normal to the plane of vectors $(\boldsymbol{\kappa} - \mathbf{g}, \boldsymbol{\kappa}) \to \sigma$-polarization, and if $\boldsymbol{\varepsilon}_{g\tau}$ is tangential to this plane $\to \pi$-polarization), and W_τ is the so-called "resonance error", which occurs in the many-wave theory of x-ray diffraction in a crystal (see for example Ref. [8]). According to Ref. [8], the value of W_τ characterizes the deviation from the Bragg direction. Here, the indices $\parallel$ and $\perp$ denote the longitudinal and transverse components of the vector parallel and perpendicular to the channeling planes and axes, respectively.

We will consider PXRC at planar channeling and assume that the channeling planes are parallel to the plane XZ and electron longitudinal motion occurs along the Z-axis, while transverse bound motion (channeling) occurs in the YZ-plane along the Y-axis. Following Refs. [1, 4], we introduce the angular coordinates θ_x and θ_y, which describe the PXRC photon wave vector deviation from the Bragg direction: $\theta_{x,y} = c(\boldsymbol{\kappa} - \boldsymbol{\kappa}_B)|_{x,y}\omega_B^{-1} = cu_{x,y}\omega_B^{-1}$ and $\mathbf{u} = (\theta_x, \theta_y)\omega_B/c$ (see Fig. 1). Here, $\omega_B = cg_d/2\sin\theta_B$ is the x-ray photon frequency that satisfies the Bragg condition, $\boldsymbol{\kappa}_B = \omega_B\mathbf{v}/v^2 + \mathbf{g}$, $\mathbf{v}$ is the vector of longitudinal electron velocity (see Fig. 1), and $g_d = 2\pi/d_p$ and d_p are the distances between the diffraction planes. Using the matrix element (1) and performing standard calculations similar to those in Ref. [4], the following formula can be derived for the PXRC angular distribution emitted by electrons captured into a quantum state n:

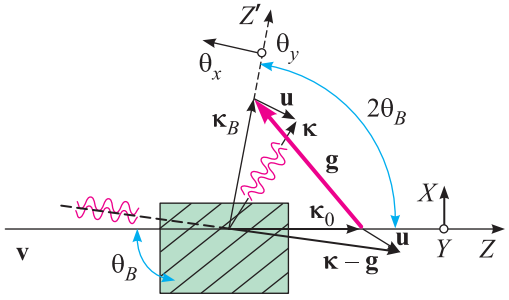

Fig. 1. Geometry of PXRC formation

$$dN^n_{\mathrm{PXRC}} = \frac{d^3N_{nn}}{d\theta_x d\theta_y dz} = dN_{\mathrm{PXR}}\,|F_{nn}|^2\,, \qquad (2)$$

where dN_{PXR} is the typical PXR angular distribution

$$dN_{\mathrm{PXR}} = \frac{\alpha\omega_B}{16\pi c\sin^2\theta_B}\left(\frac{\theta_x^2}{1+W_\pi^2} + \frac{\theta_y^2}{1+W_\sigma^2}\right), \qquad (3)$$

and F_{nn} is the form factor [4], which in the case of planar channeling can be expressed as

$$|F_{nn}|^2 = \left|\int\limits_{-d/2}^{d/2} \phi_n^*(y)\exp(-\mathbf{i}\omega_B\theta_y y/c)\phi_n(y)dy\right|^2. \qquad (4)$$

Here, $\phi_n(y)$ is the wave function for planar channeled electrons and d is the distance between the channeling planes, $\alpha = e^2/\hbar c$, and according to Ref. [4],

$$W_\tau = \frac{1}{2\,|\chi_g|\,P_\tau}\left(R - \frac{|\chi_g|^2\,P_\tau^2}{R}\right),$$
$$R = \theta_x^2 + \theta_y^2 + \theta_{\mathrm{kin}}^2,\ \theta_{\mathrm{kin}}^2 = \gamma^{-2} + |\chi_0|\,,$$
$$P_\pi = \cos 2\theta_B,\ P_\sigma = 1,\ \tau = (\pi, \sigma), \qquad (5)$$

where $\gamma = E_\parallel/mc^2$ is the relativistic factor of an electron, χ_0 and χ_g are the Fourier components of the crystal electric susceptibility.

Thus, Eq. (2) differs from the known formula for the angular distribution of PXR only by the form factor F_{nn}. The authors of Ref. [4] neglected F_{nn} in further numerical calculations. We have decided to conduct a detailed investigation of the possible influence of the form factor F_{nn} on the PXRC angular distribution.

According to formula (4), $|F_{nn}|^2 \le 1$ and $|F_{nn}|^2 \equiv 1$ if either $\theta_y = 0$ or in the dipole approximation, when $\exp(-\mathbf{i}\omega_B\theta_y y/c) \to 1$. Therefore, the PXRC intensity is always smaller than that of PXR. Furthermore, the angular distribution in the θ_y direction is expected to be different than that for PXR.

For planar channeled electrons, the longitudinal energy $E_\parallel$ is much higher than the electron transverse energy $E_\perp$, i.e. $E_\parallel \gg E_\perp$. The transverse motion of a relativistic electron in the state i can therefore be described by the wave function solution of the Schrödinger equation with relativistic mass γm [9]:

$$\left[\frac{\hat{p}_y^2}{2m\gamma} + U(y)\right]\phi_n(y) = E_{n\perp}\phi_n(y), \qquad (6)$$

where $U(y)$ is the periodic potential of the crystallographic planes.

Let us introduce the relative difference Δ_n between the PXR angular distribution and that of PXRC emitted by an electron captured into a quantum state n:

$$\Delta_n = [dN_{\mathrm{PXR}} - dN^n_{\mathrm{PXRC}}P_n(\theta_\circ)]/dN_{\mathrm{PXR}}. \qquad (7)$$

Here, $P_n(\theta_\circ)$ is the probability of an electron being captured into a sub-barrier level n (initial population of the n-th energy level), which is defined by:

$$P_n(\theta_\circ) = \frac{1}{d}\left|\int_{-d/2}^{d/2} \exp(\mathbf{i}k_y\theta_\circ y)\phi_n(y)dy\right|^2, \qquad (8)$$

where d is the distance between the channeling planes, $\theta_0 = \arctan(p_\perp/p_\parallel)$ is the angle of incidence with respect to the crystallographic plane, $p_\parallel = p_z$ and $p_\perp = p_y$ are the momentum components of an electron entering into a crystal. When $\theta_0 = 0$, the total population of all sub-barrier levels must be equal to 1.

The formula for the relative difference Δ_n is then expressed as:

$$\Delta_n = 1 - |F_{nn}|^2\, P_n(\theta_\circ). \qquad (9)$$

Thus, Eq. (9) contains two quantum corrections; the form factor F_{nn} and population $P_n(\theta_\circ)$.

Fig. 2 shows the calculated angular distribution of PXRC diffracted at the Si(1$\bar{1}$1) plane (section along the

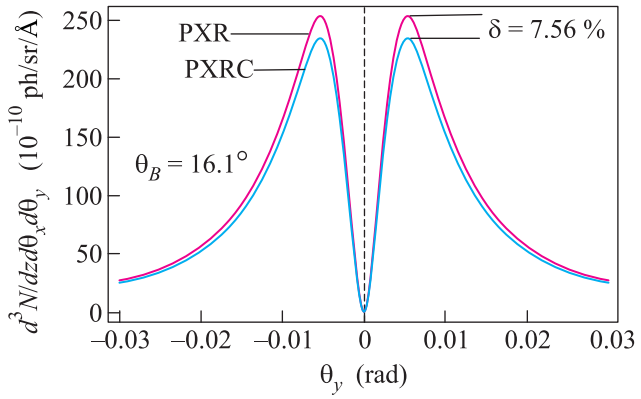

Fig. 2. Calculated PXRC and PXR angular distributions (section along the plane $\theta_x = 0$) from an electron beam with energy 255 MeV ($\gamma \simeq 500$) for Si(220) channeling (initial angle $\theta_o = 0$). Diffraction plane: (1$\bar{1}$1)

plane $\theta_x = 0$) from an electron beam with an energy of 255 MeV ($\gamma \simeq 500$) channeled in Si(220) at an initial incidence angle $\theta_0 = 0$, and the same angular distribution of PXR (random orientation). The wave functions are calculated using the model presented in Ref. [5, 6] and the angular distributions of PXRC obtained using formula (10).

The PXRC angular distribution is calculated using the following formula:

$$\frac{d^3N_{\mathrm{PXRC}}}{d\theta_x d\theta_y dz} = dN_{\mathrm{PXR}} \sum_n P_n(\theta_\circ)|F_{nn}|^2\,. \qquad (10)$$

In (10), the form factor $|F_{nn}|^2$ is calculated with "true" wave functions obtained for "true" Si(220) periodic channeling potential, as described in Refs. [5] and [6]. To characterize the relative difference of PXR and PXRC while also taking into account all populated levels, Eq. (9) may be generalized, i.e. replace $\Delta_n \Rightarrow \delta = 1 - \sum_n P_n(\theta_\circ)|F_{nn}|^2$. The value of δ is shown in Fig. 2 at the maxima of PXR and PXRC.

Thus, for a perfect electron beam (without divergence) with energy 255 MeV ($\gamma \simeq 500$) and an angle of incidence $\theta_0 = 0$, the maximal difference in the number of emitted PXRC-photons during Si(220) channeling and PXR-photons ($\theta_0 \gtrapprox \theta_L$) can reach $\delta = 7.56\,\%$. Accordingly, the case when $\theta_0 = 0$ is the best to study PXRC, because the above-barrier quantum channeling states are not populated.

Finally, we may conclude that, as expected, two quantum corrections (bound quantum states of transverse motion and their initial populations) lead to a significant decrease in magnitude and a slight narrowing in the θ_x direction of PXRC angular distribution during planar channeling.

3. The experimental observation of PXRC. Now, we present recent experimental results for PXR and PXRC obtained using a relativistic electron beam.

Fig. 3 shows a schematic of the experimental setup. The electron beam energy was 255 MeV. The beam

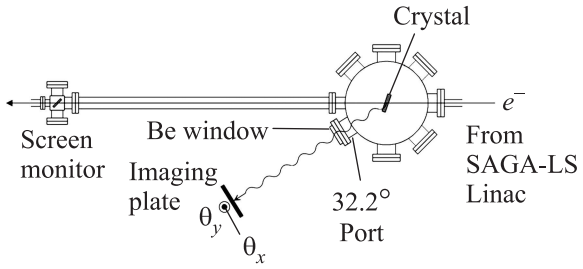

Fig. 3. Experimental setup at the SAGA-LS linac (top view)

size was (horizontal) $\sigma_x = 0.2$ mm and (vertical) $\sigma_y = 0.7$ mm, and the beam divergence was (horizontal) $\sigma'_x = 0.2$ mrad and (vertical) $\sigma'_y = 0.3$ mrad at the target position [10]. The beam divergence is smaller than the critical angle ($\theta_L = 0.41$ mrad if $U_\circ = 21.2137$ eV) for (220) planar channeling in Si. A 20 μm thick Si crystal was mounted on a two-axis goniometer in a vacuum chamber. The surface of the crystal was perpendicular to the $\langle 001\rangle$ axis. The crystal was set so that the (220) plane lay horizontally. An imaging plate (IP) ($200 \times 200\,\mathrm{mm}^2$) was used as a position-sensitive x-ray detector. IPs have many advantages, such as a large detection area, high position resolution, and high

linearity in intensity, and they are widely used in the field of x-ray imaging. The pixel size of the IP was $50 \times 50\,\mu\text{m}^2$. The IP was placed at an observation angle of $2\theta_B = 32.2°$. The distance between the crystal and the IP was 1 m. Emitted x-rays were extracted to the air through a beryllium window. The $(1\bar{1}1)$ plane was employed as a diffraction plane. In this case, the Bragg energy ($\theta_B = 16.1°$) was calculated to be 7.1 keV.

Angular distributions of x-rays emitted from the Si crystal were measured using the IP. The measurements were performed for two cases: (220) planar channeling and the "random" case when the angle of incidence was greater than the Lindhard critical angle for channeling, θ_L. The electron beam current was ~ 7 nA and the measurement time was 600 s. A typical image obtained on the imaging plate is shown in Fig. 4. The background

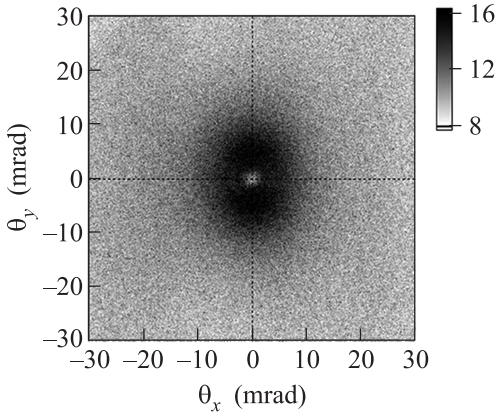

Fig. 4. Typical image obtained on the imaging plate: PXRC angular distribution in the vicinity of observation angle $2\theta_B$

level was approximately 50 % of the peak intensity. A dip was clearly observed in the center of the distribution, which is intrinsic to the PXR(C) distribution.

Fig. 5 presents sections of the image in the horizontal (θ_x) and vertical (θ_y) directions, as indicated by the dotted lines in Fig. 4. When these one-dimensional data were extracted from two-dimensional data, the intensities were averaged over an area of 20×20 pixels (1×1 mm^2) on the IP. The slight difference in PXR (random) and PXRC during Si(220) planar channeling is clearly evident in the vertical (θ_y) direction. This difference is absent in the section of the horizontal (θ_x) direction.

The theoretical ($\delta = 7.56$ %, Fig. 2) and experimental ($\delta = 6$ %, Fig. 5) values of δ that characterize the relative difference between the PXR and PXRC angular distributions along the plane $\theta_x = 0$ are in good agreement.

According to Eq. (4), the form factor $|F_{nn}|^2 \equiv 0$ for the section along the plane $\theta_y = 0$. That is, the PXR

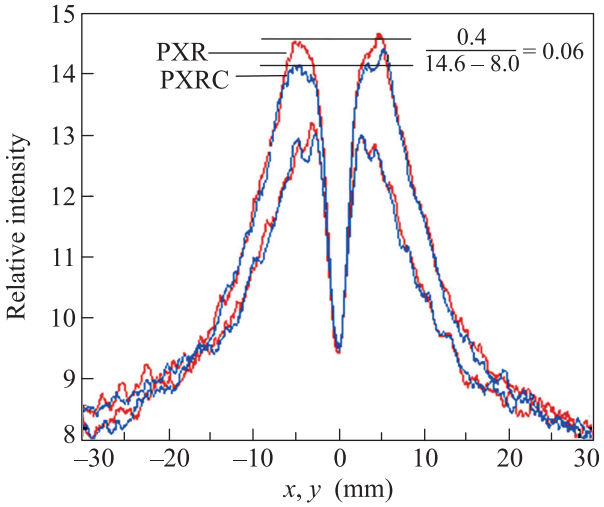

Fig. 5. Experimental data for PXRC and PXR angular distributions from an electron beam with energy 255 MeV during Si(220) channeling (upper curves – section along the plane $\theta_x = 0$, lower curves – section along the plane $\theta_y = 0$)

and PXRC angular distributions in this section do not differ. The experimental data for the PXR and PXRC angular distributions along the plane $\theta_y = 0$ are shown in Fig. 5 (lower curves). It is evident that the difference between the angular distributions of PXR and PXRC in this case is equal to zero; therefore the theoretical and experimental evidence are again in agreement.

4. Conclusions. In summary, a detailed theoretical and experimental investigation of PXRC was conducted for the first time.

The observed peculiarities in PXRC angular distributions are connected with two quantum corrections (effects); the appearance of quantum states of transverse motion electrons under channeling and the initial populations of these states.

Preparations for further experiments at the SAGA-LS linac are in progress and will include the following studies of PXRC: orientation dependence on the angle of incidence into a crystal, measurements at lower beam energy (up to 20 MeV), the use of thinner (up to 1 μm) Si crystals to avoid dechanneling, and measurements at different θ_B.

The authors are grateful to Prof. H. Nitta and Prof. M.I. Ryazanov for useful discussions.

The experimental work was supported in part by Grant-in-Aid for Scientific Research (# 21740217) from Japan Society for the Promotion of Science.

1. V. G. Baryshevsky and I. Ya. Dubovskaya, J. Phys. C: Solid State Phys. **16**, 3663 (1983).

2. T. Ikeda, Y. Matsuda, H. Nitta, and Y. H. Ohtsuki, Nucl. Instrum. Methods Phys. Res. B **115**, 380 (1996).
3. Y. Matsuda, T. Ikeda, H. Nitta et al., Nucl. Instrum. Methods Phys. Res. B **115**, 396 (1996).
4. R. Yabuki, H. Nitta, T. Ikeda, and Y. H. Ohtsuki, Phys. Rev. B **63**, 174112 (2001).
5. O. V. Bogdanov, K. B. Korotchenko, and Yu. L. Pivovarov, JETP Lett. **85**(11), 555 (2007).
6. O. V. Bogdanov, K. B. Korotchenko, Yu. L. Pivovarov, and T. A. Tukhfatullin, Nucl. Instrum. Methods Phys. Res. B **266**, 3858 (2008).
7. K. B. Korotchenko, Yu. L. Pivovarov, and T. A. Tukhfatullin, Nucl. Instrum. Methods Phys. Res. B **269**, 2840 (2011).
8. Y. H. Ohtsuki, *Charged Beam Interaction with Solids*, Taylor & Francis, London–N.Y., 1983.
9. V. A. Bazylev and N. K. Zhevago, *Radiation of Fast Particles in Matter and External Fields*, Nauka, Moscow, 1987 [in Russian].
10. Y. Takabayashi, T. Kaneyasu, and Y. Iwasaki, Nuovo Cimento C **34**(4), 221 (2011).